WISPCam: A Battery-Free RFID Camera

Saman Naderiparizi[1], Aaron N. Parks[1], Zerina Kapetanovic[1], Benjamin Ransford[2], Joshua R. Smith[2,1]
[1]Electrical Engineering Department and [2]Computer Science and Engineering Department
University of Washington, Seattle, USA-98195

***Abstract*—Energy-scavenging devices with general-purpose microcontrollers can support arbitrarily complex sensing tasks in theory, but in practice, energy limitations impose severe constraints on the application space. Richer sensing such as image capture would enable many new applications to take advantage of energy scavenging. Richer sensing faces two key challenges: efficiently retaining the necessary amount of harvested energy, and storing and communicating large units of sensor data. This paper presents the *WISPCam*, a passive UHF RFID camera tag based on the Wireless Identification and Sensing Platform that overcomes these two challenges to support reliable image capture and transmission while powered by an RFID reader. The *WISPCam* uses a novel charge-storage scheme designed specifically to match the image sensor's needs. This scheme optimally balances capacitance and leakage to improve the sensitivity and efficiency of the power harvester. The *WISPCam* also uses a novel data storage and communication scheme to reliably support the transfer of complete images to an RFID reader application. The *WISPCam* makes battery-free image capture practical for applications such as mechanical gauge reading and surveillance, both demonstrated in this paper, and opens the door to richer sensing applications on battery-free devices.**

I. Introduction

Recent research has shown that battery-free sensing is feasible with passive RFID technology. Early research-grade systems describing battery-free sensing first targeted sensing of simple quantities, such as temperature or light intensity [1], or highly targeted phenomena, such as neural signals [2] or specific motions [3]. In recent years, commercial sensing systems based on RFID technology have become available, targeting applications ranging from strain monitoring to pick-to-light systems to tire pressure monitoring for aircraft [4], [5].

A commonality with all existing RFID-based sensors is the simplicity of the sensing they support. Existing systems perform sensing either by using extremely low-power sensor modules operated at a low output data rate to conserve power, or by cleverly employing varying electrical properties of the antenna that depend on environmental quantities [6]. This simplicity is largely attributable to limited on-board energy storage. Applications requiring a high data rate, such as neural recording [2], have used small data packets that can be computed and sent just before a small on-board capacitor runs out of energy. More complex sensing reduces the effective data rate; commercial products performing sensing of simple quantities have a 1 Hz advertised output data rate and operate up to 1.5 m from an RFID reader [4].

A naïve approach to overcoming the limited sensing capabilities of battery-free platforms is to increase on-board energy storage by merely substituting a larger storage capacitor.

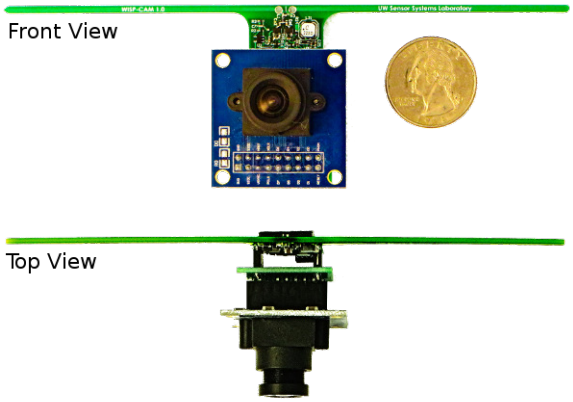

Fig. 1. The prototyped *WISPCam*, a wireless and battery-free (passive) UHF RFID camera tag. The *WISPCam* is currently implemented as a stack of three PCBs: a modified WISP 5.0 [7], an Omnivision OV7670 camera module development board, and a pin-compatibility adapter.

Greater capacitance enables longer-lasting or more energy-intensive sensing tasks, such as temperature sensing outside the range of an RFID reader [8], but naïvely integrating additional capacitance brings a significant drawback: parasitic leakage current in charge-storage devices typically *increases* with capacitance, threatening to consume an unacceptable share of an energy-scavenging platform's tight power budget.

A second challenge for richer sensing is that complex sensors typically produce large amounts of data during operation. When coupled with low-power microcontrollers that constrain RAM size to limit static power consumption, a sensor (e.g., a camera module) may produce more data than can fit in RAM. Storing to on-board *nonvolatile* memory has traditionally not been an option because writing to flash memory is prohibitively slow and energy intensive. Past systems have resorted to offloading data storage over the low-throughput backscatter link to avoid flash memory [9].

Taking these challenges into account, an energy-harvesting platform supporting complex sensing must balance charging time, application responsiveness, and richness of sensor data to meet the needs of the target application.

This paper proposes, designs and evaluates the *WISPCam*, a battery-free camera based on the Wireless Identification and Sensing Platform (WISP) [10]. In comparison with prior RFID-attached sensors, a camera is a relatively complex and power-hungry load (millijoules, not microjoules, per sensing task), and it produces a much larger amount of data (tens of KB, versus a few bytes). To meet the needs of its off-the-shelf camera component, the *WISPCam* focuses on maximizing the

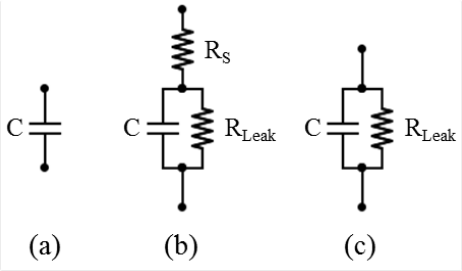

Fig. 2. Ideal supercapacitor model (a), model with parasitics (b), and simplified model neglecting R_S (c). For the employed supercapacitors, R_S is less than 1Ω [11].

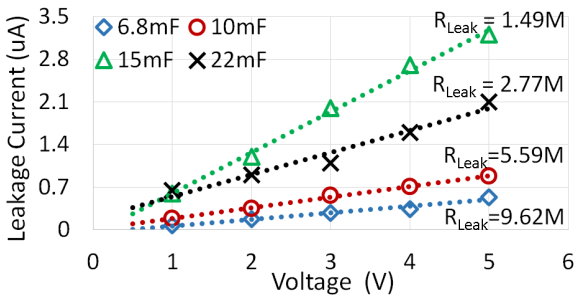

Fig. 3. Leakage currents of tested supercapacitors as a function of voltage. Leakage can be closely approximated by a simple resistive model, and extracted resistance values (R_{Leak}) are given for each device.

efficiency of large-scale energy storage and data transmission with parameters chosen to balance all of the aforementioned concerns. To support the camera's large (about 25 KB per capture for a gray scale 176*144 QCIF image frame) data size, the *WISPCam* takes advantage of newly available nonvolatile FRAM memory technology that enables quick buffering of image data for later transmission to an RFID reader. The *WISPCam* reliably transmits an image over a sequence of many smaller transmissions within the EPC Class 1 Gen 2 protocol. The *WISPCam* makes battery-free image sensing feasible for monitoring and detection applications.

Contributions. This paper makes two primary contributions in addition to the design and implementation of the *WISPCam*: (1) a charge-storage model that takes leakage into account to optimize the choice of storage capacitor, and (2) an image capture and transmission scheme tailored to battery-free sensing that leverages fast nonvolatile memory and backscatter communication.

Section II describes the design space for the system and further explores the power and data handling challenges outlined above. Section III describes specifics of the *WISPCam* prototype implementation. Section IV evaluates the prototype with respect to power consumption, energy harvesting and storage efficiency, and general performance. Section V discusses two potential applications for the *WISPCam* and presents a preliminary proof-of-concept for these two applications.

II. Design of the *WISPCam*

This section describes two major challenges in order to build a battery-free RFID camera tag like the *WISPCam*: efficiently collecting enough energy to run a rich sensor, and handling storage and transmission of a large data structure that does not fit in RAM.

A. Challenge: Efficient and Effective Charge Storage

Prior WISP-based sensing devices required tens of microjoules per sample when performing sensing tasks [1], [8]. In contrast, capturing a frame from a modern camera module requires on the order of tens of *milli*joules per image capture. Capturing an image requires a brief period of high current, resulting in power consumption far greater than the RF harvester's maximum output. Supplying enough energy for this operation is the *WISPCam*'s primary energy-storage goal.

Because a large on-board supply may take significant time to charge, minimizing leakage current is an important design goal. Excessive leakage current would hinder the platform's basic operation—even low-power operations would become high-power operations—and potentially consume energy that should be devoted to image capture.

An additional consideration is the longevity of the energy-storage element; applications in need of an RFID camera tag presumably seek a solution that does not require frequent maintenance. Supercapacitors and rechargeable batteries seem to be the best candidates for the *WISPCam*'s charge storage. However, rechargeable batteries do not last as long as supercapacitors; studies of supercapacitor longevity estimate that well over a century of operating life is achievable at room temperature and at low current [12]. Further, rechargeable batteries have the added inefficiencies of both electrical-to-chemical (charge cycle) and chemical-to-electrical (discharge cycle) energy conversion.

Unfortunately, supercapacitors are also not ideal. They typically exhibit disproportionately large leakage currents when compared to batteries with the same energy capacity, and these parasitic currents reduce the efficiency of charge storage.

Given the above concerns, the main question is how to most efficiently accumulate a high level of charge on leaky capacitors via potentially slow RF harvesting.

The first step in designing with leaky capacitors is to understand the system's power budget to evaluate the impact of leakage current. We expect the *WISPCam* to be capable of harvesting hundreds of microwatts of power from the RFID reader's carrier, and to be consuming tens of microwatts to tens of milliwatts depending on the operation taking place. The next step is to find a supercapacitor that has an appropriately small parasitic conductivity. Figure 3 shows the effective parallel DC resistance and leakage power consumption of several candidate supercapacitors we measured. while the voltage across supercapacitor is below 4V, each exhibits leakage power consumption of under 12 μW, two orders of magnitude smaller than the gap between expected harvester average output power and sleep-mode power consumption of the WISP's microcontroller, and are therefore reasonable choice for the energy storage component in our design.

To power its camera module, the *WISPCam*'s capacitor must charge to an upper threshold V_{max} via RF harvesting, then discharges until it reaches a minimum operating voltage V_{min}. The amount of energy transferred by the capacitor to the system during the discharge cycle—in this case, the energy

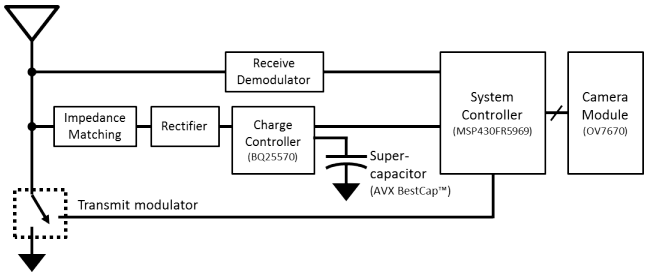

Fig. 4. *WISPCam* block diagram. A Texas Instruments MSP430 microcontroller with 64K of integrated FRAM memory implements the system controller. DC-DC conversion, supercapacitor charging, and efficient switch-mode load regulation is handled by a TI BQ25570 power management IC. The backscatter uplink and R=>T downlink demodulator are based on those employed by the WISP 5.0 [7].

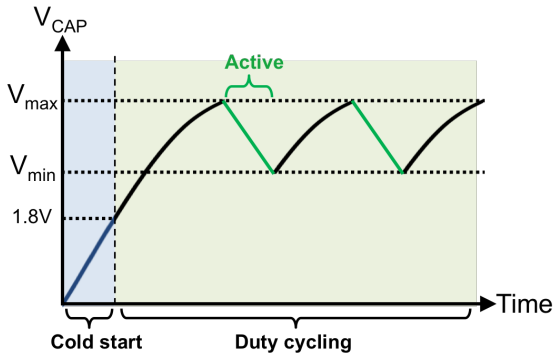

Fig. 5. Like most energy harvesting systems, the *WISPCam* operates in a duty-cycled fashion, charging a storage capacitor up to a maximum voltage V_{max} before activating. The system remains active until the capacitor voltage falls to V_{min}. In this work, the leakage energy during the charging cycle is used as a cost function for optimization.

required to capture and transmit a photo—must match the energy requirement of the load.

The energy stored in a capacitor is related to its terminal voltage as well as its capacitance. Therefore, the same energy may be stored by choosing a larger capacitor and lower V_{max} threshold, or by choosing a smaller capacitor and a higher V_{max}. Because supercapacitor leakage is approximately resistive in nature, a higher V_{max} threshold voltage means more leakage power. However, higher capacitance *also* increases leakage current. Thus, the tradeoff between capacitance and voltage threshold must be carefully weighed to determine the optimal parameters for high charge-storage efficiency.

Simplified non-ideal supercapacitors can be modeled as in Figure 2 [13]. In this work we use model (c), as the serial resistance is negligible at low current. Further, we assume that incoming power is less than required operating power, forcing the system to duty cycle. The appropriate supercapacitor is the one that minimizes energy dissipation per charging operation within the minimum and maximum voltage thresholds. The relevant parameters in our model are as follows:

- E_{load}: required energy per sensing operation;
- V_{min}: minimum voltage threshold, greater than or equal to the platform's minimum operating voltage;
- V_{max}: maximum voltage threshold, calculated using equation 1;
- C: capacitance of the supercapacitor;
- R_{Leak}: leakage parallel resistance of the supercapacitor, from datasheet or empirical measurement;
- P_{in}: input power after RF–DC and DC–DC conversion, assumed to be constant in each experiment.

In each operating cycle, the supercapacitor will discharge from voltage V_{max} down to V_{min}, as shown in Figure 5. So V_{max} can be calculated as follows:

$$E_{load} \approx \frac{1}{2}C(V_{max}^2 - V_{min}^2)$$

$$V_{max} = \sqrt{\frac{2E_{load}}{C} + V_{min}^2} \tag{1}$$

We then work towards computing the amount of energy dissipated by the parasitic leakage path in the supercapacitor over the entire charging cycle. This will be a function of the input power, as faster charging means less overall energy wastage:

$$P_{Leak} = \frac{v^2}{R_{Leak}} \Rightarrow E_{Leak} = \int_{t_{min}}^{t_{max}} P_{Leak}(t)\,dt. \tag{2}$$

Substituting dt with $\frac{C}{i}dv$,

$$E_{Leak} = \int_{V_{min}}^{V_{max}} P_{Leak}(v)\frac{C}{i_c}dv. \tag{3}$$

Assuming the input power after RF–DC and DC–DC conversion is a constant P_{in}, and using $i_c = \frac{P_{in}}{v} - \frac{v}{R_{Leak}}$,

$$E_{Leak} = \frac{C}{R_{Leak}}\int_{V_{min}}^{V_{max}} \frac{v^2}{\frac{P_{in}}{v} - \frac{v}{R_{Leak}}}dv. \tag{4}$$

For the supercapacitor charge to increase, it is required that supercapacitor leakage power is less than the total input power: $P_{in} > \frac{v^2}{R_{Leak}}$. Finally, using a simplifying substitution $U = \frac{1}{P_{in}R_{Leak} - v^2}$ and defining $U_{min} = \frac{1}{P_{in}R_{Leak} - V_{min}^2}$ and $U_{max} = \frac{1}{P_{in}R_{Leak} - V_{max}^2}$ we will have:

$$E_{Leak} = \frac{C}{2}\left(P_{in}R_{Leak}\ln\left(\frac{U_{max}}{U_{min}}\right) + \frac{1}{U_{max}} - \frac{1}{U_{min}}\right). \tag{5}$$

Equation 1 assumes that energy dissipated by the load is far more than the energy dissipated by R_{Leak} while the capacitor is discharging. In other words, the leakage energy is negligible during discharging (since leakage power is small), thus approximately the total leakage energy dissipates just during the charging cycle. This will be valid in cases where the active period is much smaller than the charge period; in other words, most high-energy loads will behave in this way. Considering active mode capacitor leakage energy is

TABLE I. COMPARING CAPACITOR LEAKAGE ENERGY DURING CHARGE CYCLE

	6.08 mF	**11.24 mF**	**17.45 mF**	**21.98 mF**
Capacitor's Rated Voltage	15V	12V	5.5V	9V
Measured R_{Leak}	9.62 MΩ	5.59 MΩ	1.49 MΩ	2.77 MΩ
Selected V_{max} for E_{load}=20 mJ	3.80V	3.38V	3.18V	3.11V
E_{Leak} @ P_{in} = 10 uW	2.63 mJ	4.18 mJ	31.03 mJ	9.26 mJ
E_{Leak} @ P_{in} = 100 uW	0.23 mJ	0.35 mJ	1.28 mJ	0.65 mJ
E_{Leak} @ P_{in} = 1 mW	0.023 mJ	0.034 mJ	0.121 mJ	0.063 mJ

difficult because it requires full time-domain characterization of the load power requirements and the capacitor's charge state during active periods.

In equation 4, t_{min} and t_{max} are the time the supercapacitor begins charging from V_{min} and the time its voltage reaches V_{max}, respectively.

To select the optimum supercapacitor, we calculate V_{max} and R_{Leak}, then use equation 4 to find E_{Leak}. The capacitor that minimizes E_{Leak} during the charging period is the most efficient one. Table I summarizes these data for our candidate supercapacitors, assuming $V_{min} = 2.8\,\mathrm{V}$, $E_{Load} = 20\,\mathrm{mJ}$, and all capacitors are charged with the same input power. The table I shows that if the charging power of the supercapacitor is high (around 1 mW), then the leakage current impact on the overall efficiency will be negligible (less than 1%). On the other hand, for low charging powers (around 10 uW) improper selection of supercapacitor may have a huge impact on the overall efficiency of the system and may turn into a limiting factor for minimum sensitivity. Our experimental results on the efficiency of power harvester (see 9) justify this table's results. Based on 9 the efficiency of the *WISPCam* when a 17.45 mF supercapacitor is connected to the output of its power harvester drops drastically once the input power is low. As a conclusion, the table shows that the 6.08 mF supercapacitor is the best candidate among those we tested.

RF power harvesting considerations: Additionally, it is desirable to have a power harvester that can dynamically track the maximum power point, since the impedance of the charge storage element is changing and charging simultaneously.

As discussed before, we decided to use a supercapacitor with millifarads capacitance as the charge storage element. The *WISPCam*'s microcontroller and camera require voltages above 2.5 V to operate properly, so the employed supercapacitor must charge up to at least this level, meaning the load connected to the power harvester is changing significantly during charging. In this case, in order to get the most out of the input RF signal, it is important to be able to adaptively change the current drawn from the rectifier's output to keep the input impedance of the system matched to the antenna as much as possible. Otherwise, energy-harvesting efficiency will be poor. To work around this challenge we used a TI boost charger that performs Maximum Power Point Tracking (MPPT) to increase the efficiency during charging.

B. Challenge: Large-Scale Data Capture and Transfer

Given a platform like the *WISPCam* that captures images on behalf of an RFID-based application, a primary design point is to ensure that image data can reach the application. Unfortunately, large-scale (tens of KB) storage and transmission are complicated for this class of devices.

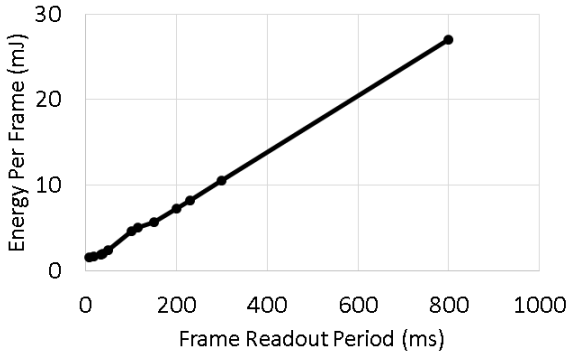

Fig. 6. Camera per frame energy consumption vs frame readout period

To minimize static power consumption due to memory, microcontrollers suitable for energy-harvesting devices typically have at most a few KB of RAM [10], [14], not enough to hold a complete image larger than 100×100 pixels. Streaming image data directly to an RFID reader during capture is infeasible because of the poor performance of RFID protocols for large-scale streaming [15], and because energy shortfalls can cause the entire platform, including sensors, to lose power mid-transfer. The remaining option is nonvolatile memory on board the sensor platform. Unfortunately, the ubiquitous flash memory in microcontrollers is too slow ($\sim 1\,\mathrm{s}$ per 10 KB), too cumbersome to write (awkward erase-before-write requirements), too energy intensive ($0.1\,\mu$J/byte [16]), and too limited in durability to be practically useful for buffering of large sensor data [17].

Figure 6 illustrates the importance of data-handling speed for the *WISPCam*. The figure shows the energy required by the camera to capture one image frame against the time required to buffer the frame to nonvolatile memory. Since the camera is the most power-hungry component of the *WISPCam*, the optimal strategy is to turn on the camera, capture a frame, transmit the frame data to memory, and then put the camera in sleep mode before transmitting to a reader.

As an alternative to flash, the *WISPCam* is built on a microcontroller that includes ferroelectric RAM (FRAM). FRAM is superior to flash by orders of magnitude along all of the dimensions described above. Using FRAM instead of flash enables a 48 Mbps transfer speed on the *WISPCam*'s microcontroller—fast enough to transfer a camera image to nonvolatile memory before exhausting the capacitor's supply. Section III gives more details on the parts involved.

III. PROTOTYPE IMPLEMENTATION

We categorize the implementation of the whole system into two sections, hardware implementation and firmware/software implementation. Most of the control logic for each module of our design is implemented in firmware, as well as the EPC Class 1 Generation 2 (EPC C1G2) protocol for UHF RFID tags which allows communication with the reader. The hardware section focuses on the power subsystem, which provides the energy harvesting and storage necessary to operate the camera tag while creating a communication infrastructure.

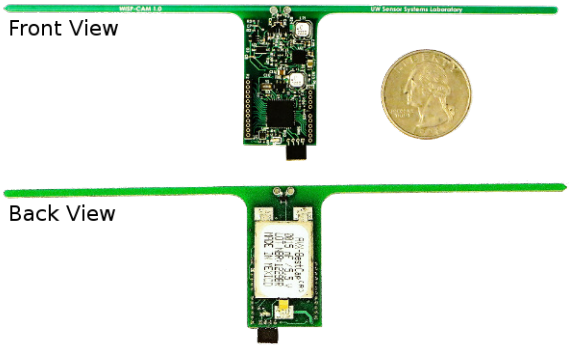

Fig. 7. *WISPCam* main board, based heavily on the WISP 5.0 [7]. An AVX BestCap series supercapacitor allows the *WISPCam* to accumulate the 20 mJ necessary for image capture and transfer.

A. Hardware implementation

Figure 4 shows the block diagram of the *WISPCam*. The harvesting system consists of an antenna to intercept RF signals produced by an RFID reader, a discrete impedance matching network, an RF-DC conversion stage utilizing the Avago HSMS-285C Schottky barrier diodes in a single-stage RF Dickson charge pump configuration, and a high-efficiency DC-DC boost conversion stage making use of a Texas Instruments BQ25570. Charge is stored on a supercapacitor chosen from the BestCap series by AVX.

Downlink communication (reader to tag) is accomplished through the use of an envelope detector and power-gated ASK demodulator circuit. The output of the demodulator is connected to the logic controller, a Texas Instruments MSP430FR5969 microcontroller. The microcontroller runs open source firmware [7] to interpret the EPC C1G2 protocol and issues responses to reader queries. Responses are transmitted via backscatter communication by modulating the impedance presented to the antenna through the transmit modulator switch shown.

1) Sensing load: Camera: The sensing load of this device is a camera, a very generally applicable sensor which requires a lot of energy per operation and is a source of a relatively large amount of data when compared with the typical byte-size quantities recorded by prior battery-free sensing loads.

We employ the OV7670 camera module due to its wide commercial availability. The nominal operating voltage for this camera is 2.8 Volts. Although the employed microcontroller, which is TI MSP430FR5969, can operate at as low as around 2 V, we choose to apply the same 2.8V to the microcontroller to eliminate the need for level shifting on the large parallel data bus which connects the microcontroller and camera.

2) Meeting energy requirements: The BQ25570 boost charger IC operates in a power cycling mode, in which charge is accumulated on the storage capacitor until and upper threshold voltage (V_{max}) is breached, then discharged through the output regulator until a lower threshold voltage is attained (V_{min}). The output regulator is also a switch-mode regulator designed for low-power loads, and maintains a far higher efficiency than the linear regulator often used in low power and energy harvesting systems [18].

Based on empirical data presented in Figure 10, we found that at least 10 mJ of energy is required to capture and store a 176*144 pixel (QCIF) gray scale image such as those seen in Figure 12 (Images with higher contrast or higher resolution will require expending more energy). We select a 6.08 mF supercapacitor and target 20 mJs of usable energy. This will ensure that the entire atomic imaging, parallel data read-out by the microcontroller, and storage operation can be finished in one active period, a requirement for successful image capture. We set V_{min} to 2.8V; to achieve 20 mJ of charge storage, by Equation 1 we select $V_{max} \approx 3.8$V.

3) Maximum power point tracking: As discussed in Section II, because of changing load it is important to have a power harvester that uses Maximum Power Point Tracking (MPPT). MPPT effectively performs DC impedance matching of the RF–DC source to the DC–DC converter's input, even as the charge storage device's effective impedance changes throughout the charge cycle. This DC impedance match is reflected by a lowered S11 magnitude at the RF input side. The boost charger, with its built-in MPPT feature, resulted in an S11 magnitude better than -25 dB over the entire supercapacitor charging cycle for RF input powers smaller than -12 dBm.

B. Firmware implementation

Firmware running on the microcontroller initializes the camera, triggers the shutter, and receives image frame data through an eight-bit parallel bus (clocked at 6 MHz) and several control lines.

The *WISPCam*'s MSP430FR5969 microcontroller has a 64KB on-chip FRAM memory that supports 48 Mb/s data transfer from the camera to the microcontroller while burning only a few milliwatts of power. The *WISPCam* uses the DMA module of the MSP430 to perform this high-speed transfer of image data to FRAM without the intervention of CPU.

1) Host-side application: Communication between the *WISPCam* and a host computer takes place through a commercial-off-the-shelf RFID reader (Impinj Speedway R1000). We developed a host-side application that relies on an open-source Python library for interfacing with RFID readers [19]. This application implements a simple transfer protocol with the *WISPCam*, listening for image data and requesting missing or corrupted packets if errors occur during transfer. Image data is transferred through EPC modulation [1], in which certain fields of the electronic product code (EPC) of the RFID tag being emulated by the *WISPCam* contains the data payload from the camera.

2) Saving state: The *WISPCam* implements a hibernation state in which critical status information is saved to non-volatile memory prior to a power loss event. For instance, the *WISPCam* maintains the address of the next image pixel to be transmitted. If execution is interrupted, the *WISPCam* can resume transmission from nonvolatile memory.

C. WISPCam Prototype

Figure 1 shows the actual prototyped *WISPCam* which is an Omnivision OV7670 VGA camera board on top of a modified WISP 5.0. Figure 7 illustrates the front and back

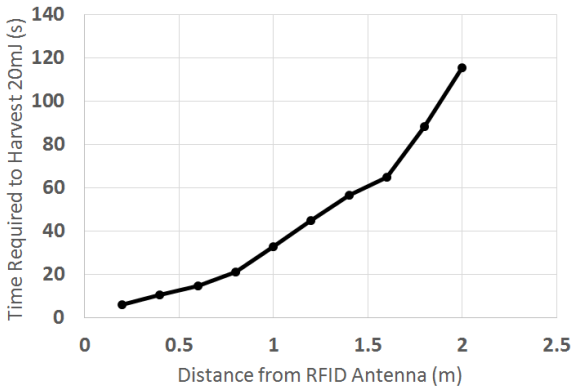

Fig. 8. Time required to harvest 20 mJ versus the distance between the *WISPCam* and the RFID reader. A 9dBic circularly polarized antenna was used as the reader antenna and a 1 W power level was set at the reader, making for 4 W EIRP for the *WISPCam*'s linearly polarized antenna.

view of the modified WISP 5.0 board. The employed 6.08 mF supercapacitor is soldered on the back side of the modified WISP 5.0 and takes up almost all the space on the bottom side.

IV. Results

This section presents the results of three different experiments we performed to measure the performance and power consumption of the *WISPCam*.

The first experiment's goal is to evaluate efficiency of the power harvester while harvesting from a continuous RF 915 MHz signal. The *WISPCam*'s boost charger unfortunately exhibits poor cold-start performance. The boost charger will be in a cold-start state as long as the voltage across the supercapacitor is less than 1.8V. The minimum sensitivity of the system to do a cold start is about -12.1dBm, although this will improve due to MPPT once supercapacitor voltage is above 1.8V (past cold start). In this experiment, we measured the capacitance of four different supercapacitors from AVX by connecting them to a Source Measure Unit (SMU) and reading the slope of rising voltage while providing them with constant current. The nominal values are 6.8 mF, 10 mF, 15 mF and 22 mF whereas the measured capacitances are 6.08 mF, 11.24 mF, 17.45 mF and 21.98 mF accordingly. Then, we connected these four supercapacitors to the output of the power harvester one at a time. The RF input power changed from -12.1 dBm to 8.9 dBm and the supercapacitors in each of the four cases were charged from 2V to 3.8V. Using LabVIEW data acquisition, we logged time-domain charging information to a file and measured efficiency based on equation 6, where Δt is the total charge time (charging from 2V to 3.8V). Figure 9 shows the efficiency curves of the different supercapacitors. From this figure we can see that by using a 6.08 mF supercapacitor for lower input power, we can achieve more than 23% efficiency, and this trend will increase while the input power increases to some extent, further increase in the input power will result in decreasing the efficiency.

$$\eta(\%) = 100\frac{\frac{1}{2}C(3.8^2 - 2^2)}{P_{in}\Delta t} = 100\frac{5.22C}{P_{in}\Delta t} \qquad (6)$$

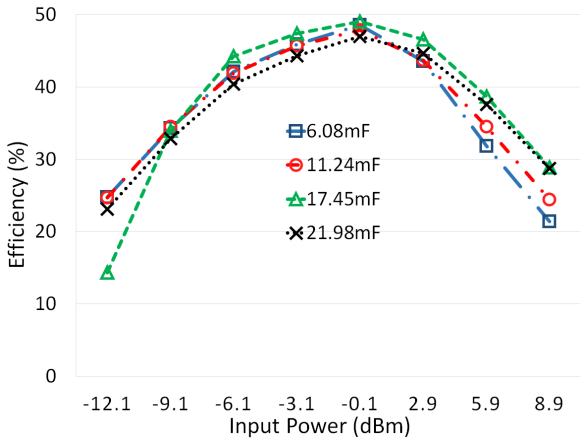

Fig. 9. Energy efficiency of the power harvester when charging four different supercapacitors from 2V to 3.8V

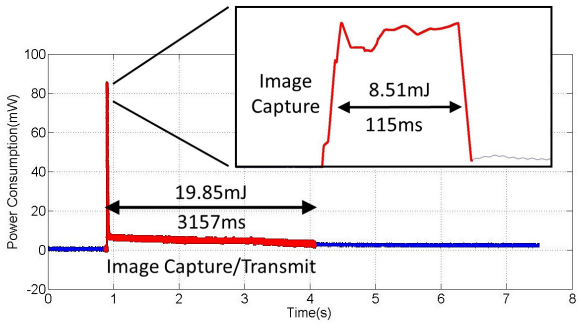

Fig. 10. Time domain *WISPCam* power consumption while capturing, storing and transmitting the image

The second experiment measures the *WISPCam*'s power consumption of the system in the time domain for both image capturing/storage (camera and microcontroller in active mode) and image transferring (camera in low-power mode and microcontroller in active mode). As Figure 10 shows, initially the system is not powered, and therefore the power consumption is zero. Once powered on, the system enters the image-capturing state, where power consumption spikes for 115 ms. During this phase the *WISPCam* burns about 8.51 mJ. After it is done with image capturing/storage, it enters the image-transfer state where the camera is no longer in active mode. This phase lasts about 3 s and the *WISPCam* consumes 11.34 mJ during that. The overall process takes about 3.2 s and the *WISPCam* burns 19.85 mJ over one entire image capturing, storing and transmission process.

The third experiment evaluates the performance of the *WISPCam* prototype in terms of distance from an RFID reader which transmits 1 W of RF power and is connected to a 9dBic circularly polarized antenna. Figure 8 shows that as the distance from the antenna increases, the power harvester requires more time to harvest 20 mJ, as expected. Based on this figure, if the *WISPCam* is 20 cm away from the RFID antenna in a single-tag environment, it will emit a new picture captured and transmitted approximately every 10 seconds. It is important to note that our experiments show that in a single tag environment, the *WISPCam* works up to 5 m away

Fig. 11. The *WISPCam*, mounted on an industrial gas cylinder, monitors a pressure gauge.

from the RFID antenna and captures and transmits an image approximately every 15 minutes.

V. Applications

The *WISPCam* allows for battery-free imaging by harvesting wireless power and using low-power backscatter communication to both capture and transmit images. The major significance of the *WISPCam* is its ability to capture images without the limitations of batteries, excess wiring, or complex installation, while still remaining a low-power system. These functions and features introduce many promising real-world applications for the *WISPCam*.

The device can be used for applications such as monitoring inaccessible areas or general surveillance (e.g., home security). For instance, in the microelectronics industry, there are semiconductor fabrication plants that utilize numerous analog gauges. These analog gauges are often located in hard-to-reach places and require frequent monitoring. The *WISPCam* can be an effective solution for this application because it is completely battery-free and wireless, resulting in a very low-maintenance and cost-efficient system. Similarly, monitoring analog gauges on gas tanks can be useful—for example, surveying an analog pressure gauge on a helium tank to determine when a replacement is needed.

In order to demonstrate the potential for these two applications and many others, we developed a software interface to communicate with the *WISPCam* and display captured images in real time, as shown in Figure 13. We implemented the interface in Python using various software libraries, including a pure-Python LLRP library [19]. We mounted the camera in front of an analog gauge, shown in Figure 11, with an Impinj reader and an antenna nearby. The reader was connected to a PC with the software interface configured to display the captured images of the analog gauge. These images are shown in Figure 12.

Another application for the camera is in the field of security and surveillance. The *WISPCam* is advantageous compared to current surveillance systems because it is wireless and battery free. These are appealing features because they eliminate potential scenarios such as power disconnection that would disable the system. Additionally, we integrated a Passive Infrared (PIR) motion sensor with the *WISPCam* to trigger

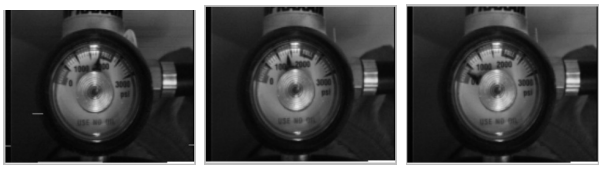

Fig. 12. A mechanical pressure gauge as captured by the *WISPCam* using the setup in Figure 11. These images could be post-processed to extract the gauge reading, or displayed directly to a human operator.

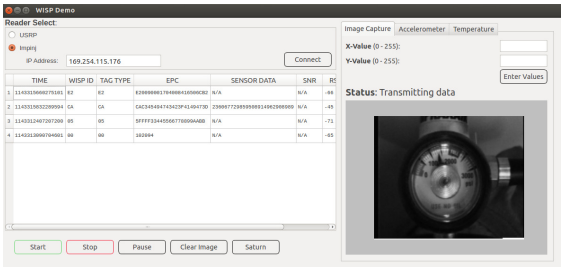

Fig. 13. A *WISPCam* host application with GUI handles data transfer and image display.

the capture of an image only when movement is detected. To integrate the motion detector, we implemented a simple circuit that consumes a negligible amount of power (about 10 uW) using the *WISPCam*'s harvested energy and uses the output signal from the motion sensor as a trigger to enable the *WISPCam*. This feature can be useful in environments that require monitoring unexpected changes in the surroundings. To validate the integration of the PIR motion sensor, we used the software interface to collect captured images from the *WISPCam* triggered by the sensor, shown in Figure 14.

The *WISPCam* would also be beneficial in aircraft inspection. All airlines are required to have a maintenance plan that schedules the regular maintenance of each airplane in the fleet. Typically, these inspections occur monthly and involve opening areas of the aircraft that are somewhat inaccessible [20]. Many of these maintenance checks are overnight activities, however they can also have a duration of 20 to 30 days [20]. Installing the *WISPCam* in areas of an aircraft that require frequent and extensive inspection would allow for more constant monitoring and potentially improve the efficiency and safety of airline maintenance plans.

VI. Conclusion

This paper presented the *WISPCam*, a battery-free camera based on a modified WISP 5.0, and addressed the challenges around harvesting large amounts of energy and handling large amounts of data on a transiently powered platform. We presented a method for selecting an optimal supercapacitor from a set of real supercapacitors given a load energy requirement and an input power. This method is generally applicable to systems operating high-energy loads in energy-harvesting scenarios.

The *WISPCam* was able to cold-start and operate at -12.1 dBm RF input power, storing 20 mJ of energy on a supercapacitor. Once started, the *WISPCam* was able to operate down to -15 dBm input power. The *WISPCam* successfully and repeatedly captured and transmitted images to a host ap-

Fig. 14. A person passing through a doorway triggers a PIR sensor mounted on the *WISPCam*, which then captures an image of the scene.

plication via a commercial-off-the-shelf RFID reader, proving the feasibility of a battery-free camera system.

Example applications demonstrated include gauge reading and surveillance. However, a camera sensor is widely applicable to a variety of sensing applications, making this one of the first generally applicable battery-free sensing systems.

REFERENCES

[1] A. Sample and J. Smith, "Experimental results with two wireless power transfer systems," in *Radio and Wireless Symposium, 2009. RWS '09. IEEE*, pp. 16–18, 2009.

[2] D. Yeager, J. Holleman, R. Prasad, J. Smith, and B. Otis, "Neuralwisp: A wirelessly powered neural interface with 1-m range," *IEEE Transactions on Biomedical Circuits and Systems*, vol. 3, pp. 379–387, Dec. 2009.

[3] M. Buettner, R. Prasad, M. Philipose, and D. Wetherall, "Recognizing daily activities with RFID-based sensors," in *UbiComp*, Sept. 2009.

[4] "Farsens battery-free sensor solutions." http://www.farsens.com/en/battery-free-sensor-solutions. Accessed December 2014.

[5] "Tire pressure and brake temperature systems – smartstem." http://www.craneae.com/Products/Sensing/SmartStem.aspx. Accessed December 2014.

[6] A. Sample, D. Yeager, and J. Smith, "A capacitive touch interface for passive rfid tags," in *RFID, 2009 IEEE International Conference on*, pp. 103–109, Apr. 2009.

[7] "Wisp 5 firmware repository." http://www.github.com/wisp/. Accessed December 2014.

[8] D. J. Yeager, P. S. Powledge, R. Prasad, D. Wetherall, and J. R. Smith, "Wirelessly-charged UHF tags for sensor data collection," in *RFID, 2008 IEEE International Conference on*, pp. 320–327, IEEE, 2008.

[9] M. Salajegheh, S. S. Clark, B. Ransford, K. Fu, and A. Juels, "CCCP: secure remote storage for computational RFIDs," in *Proceedings of the 18th USENIX Security Symposium*, (Montreal, Canada), pp. 215–230, Aug. 2009.

[10] J. R. Smith, A. P. Sample, P. S. Powledge, S. Roy, and A. Mamishev, "A wirelessly-powered platform for sensing and computation," in *UbiComp 2006: Ubiquitous Computing*, pp. 495–506, Springer Berlin Heidelberg, 2006.

[11] "Avx bestcap datasheet." http://www.avx.com/docs/Catalogs/bestcap.pdf.

[12] S. Kim and P. H. Chou, "Size and topology optimization for supercapacitor-based sub-watt energy harvesters," *Power Electronics, IEEE Transactions on*, vol. 28, pp. 2068–2080, Apr. 2013.

[13] A. Weddell, G. V. Merrett, T. Kazmierski, and B. Al-Hashimi, "Accurate supercapacitor modeling for energy harvesting wireless sensor nodes," *Circuits and Systems II: Express Briefs, IEEE Transactions on*, vol. 58, pp. 911–915, Dec. 2011.

[14] Y. Yan, D. Wu, H. Liu, L. Pan, and J. Xu, "A pure logic cmos based low power non-volatile random access memory for rfid application," in *ASIC, 2009. ASICON '09. IEEE 8th International Conference on*, pp. 1015–1018, Oct. 2009.

[15] S. Thomas, T. Deyle, R. Harrison, and M. Reynolds, "Rich-media tags: Battery-free wireless multichannel digital audio and image transmission with uhf rfid techniques," in *RFID (RFID), 2013 IEEE International Conference on*, pp. 231–236, Apr. 2013.

[16] G. Mathur, P. Desnoyers, P. Chukiu, D. Ganesan, and P. Shenoy, "Ultra-low power data storage for sensor networks," *ACM Trans. Sen. Netw.*, vol. 5, pp. 33:1–33:34, Nov. 2009.

[17] "MSP430 flash memory characteristics." http://www.ti.com/lit/an/slaa334a/slaa334a.pdf. Accessed December 2014.

[18] "Bq25570 datasheet." http://www.ti.com/product/BQ25570/datasheet/.

[19] "sllurp – Python client for LLRP-based RFID readers." https://github.com/ransford/sllurp. Accessed December 2014.

[20] "Human factors issues in aircraft maintenance and inspection." http://www.faa.gov/, Oct. 1989. Accessed December 2014.